Original articles

Neopepsee: accurate genome-level prediction of neoantigens by harnessing sequence and amino acid immunogenicity information

S. Kim[1,†]. H. S. Kim[2,3,†], E. Kim[1], M. G. Lee[2], E. Shin[4], S. Paik[1,3], S. Kim[1,*]

[1] Severance Biomedical Science Institute, Brain Korea 21 PLUS Project for Medical Sciences, Yonsei University College of Medicine, Seoul 03722, Korea
[2] Department of Pharmacology, Pharmacogenomic Research Center for Membrane Transporters, Brain Korea 21 PLUS Project for Medical Sciences, Yonsei University College of Medicine, Seoul 03722, Korea
[3.] Yonsei Cancer Center, Division of Medical Oncology, Department of Internal Medicine, Yonsei University College of Medicine, Seoul 03722, Korea
[4.] Graduate School of Medical Science and Engineering, KAIST, Daejeon 34141, Korea

* Correspondence to: Prof. Sangwoo Kim, Severance Biomedical Science Institute, Yonsei University College of Medicine, Seoul 120-752, Korea. Tel: +82 2 2228 0913; Email: swkim@yuhs.ac

† These authors contributed equally to this work.

KEY MESSAGE

Tumor-specific mutations create neoantigens that elicit T-cell responses. Although identifying neoantigens is crucial for developing personalized cancer immunotherapies, accurate neoantigen prediction remains a daunting problem. Here, we present a new machine-learning based method incorporating nine features related to immune response. Our approach paves the way for improving neoantigen discovery.

ABSTRACT

Background: Tumor-specific mutations form novel immunogenic peptides called neoantigens. Neoantigens can be used as a biomarker predicting patient response to cancer immunotherapy. Although a predicted binding affinity (IC_{50}) between peptide and major histocompatibility complex class I (MHC-I) is currently used for neoantigen prediction, large number of false-positives exist.

Materials and methods: We developed Neopepsee, a machine learning-based neoantigen prediction program for next-generation sequencing data. With raw RNA-seq data and a list of somatic mutations, Neopepsee automatically extracts mutated peptide sequences and gene expression levels. We tested 14 immunogenicity features to construct a machine-learning classifier and compared with the conventional methods based on IC_{50} regarding sensitivity and specificity. We tested Neopepsee on independent data sets from melanoma, leukemia, and stomach cancer.

Results: Nine of 14 immunogenicity features that are informative and inter-independent were used to construct the machine-learning classifiers. Neopepsee provides a rich annotation of candidate peptides with 87 immunogenicity-related values, including IC_{50}, expression levels of neopeptides and immune regulatory genes (e.g., PD1, PD-L1), matched epitope sequences, and a three-level (high, medium, and low) call for neoantigen probability. Compared to the conventional methods, the performance was improved in sensitivity and especially 2- to 3-fold in the specificity. Tests with validated datasets and independently proven neoantigens confirmed the improved performance in melanoma and chronic lymphocytic leukemia. Additionally, we found sequence similarity in proteins to known pathogenic epitopes to be a novel feature in classification. Application of Neopepsee to 224 public stomach adenocarcinoma datasets predicted ~7 neoantigens per patient, the burden of which was correlated with patient prognosis.

Conclusions: Neopepsee can detect neoantigen candidates with less false positives and be used to determine the prognosis of the patient. We expect that retrieval of neoantigen sequences with Neopepsee will help advance research on next-generation cancer immunotherapies, predictive biomarkers, and personalized cancer vaccines.

Keywords: Cancer, Classification, Immunoinformatics, Neoantigen, Next-generation sequencing

INTRODUCTION

Somatic mutations can cause tumor-specific neopeptide fragments (so-called "neoantigens"), some of which induce cytotoxic T cell responses [1]. Importantly, neoantigen prediction can be exploited to identify responders to immune checkpoint inhibitors [2-4]. Therefore, systematic evaluation of somatic mutations may help advance the promising clinical outcomes of immunotherapies in cancer treatment.

For a somatic mutation to be recognized by cytotoxic T cells, the mutant peptide should be presented by major histocompatibility complex class I (MHC-I) molecules [5] (Figure 1A). First, mutant proteins are cut into short peptides by proteasomes and then transported into the endoplasmic reticulum by the transporter associated with antigen processing (TAP). When mutant peptide binds to the MHC-I peptide-binding groove, fully assembled peptide-MHC-I complexes (pMHC-I) are presented at the surface of the plasma membrane. The recognition of a neoantigen by a cytotoxic T cell can activate the T cell response.

To date, most *in silico* approaches for neoantigen prediction have been focused on the MHC-I related presentation of peptides [6, 7]. Because only 0.5% of peptides can bind to MHC-I molecules, prediction of the binding affinity is the most selective step in the recognition of endogenous antigens [8]. Although these tools provide reliable measurements, practical application at the genome-level is limited. First, the prediction of immunogenic neoantigens primarily relies on a single arbitrary cut-off (50 or 500nM) of a predicted MHC-I binding affinity. Second, isoform-specific gene expression levels of putative neoantigens and other immune signature-related genes are mostly not estimated or considered. Third, the actual analysis requires a series of complex computational processes, which should be handled by bioinformatics experts manually.

Here, we describe a new machine-learning based method to address the noted problems above and its implementation. The program, called Neopepsee, harnesses gene- and protein-level information and a novel feature to achieve maximum accuracy: improved performance was validated in a cross validation and an independent *in vivo* study.

MATERIAL AND METHODS

Collection of potential immunogenicity features

To build a classifier that maximizes the usage of information, we initially collected 13 potential features that have been previously reported or hypothesized for predicting immunogenicity. The 13 potential features were divided into three groups based on their representative biological meanings: (A)

MHC-I binding and presentation, (B) amino-acid characteristics, and (C) complex scores. For (A), seven features have been collected and scored, including IC_{50} and *percentile rank* based predictive values for MHC-I binding affinity, NetCTLpan [9] based scores for *MHC-I binding*, *protein cleavage*, *TAP transport efficiency* and their *combined score*. A score for *T-cell recognition* of the pMHC-I molecule [10] was also considered. For (B), four features have been collected including *hydrophobicity* of amino acids at TCR contact residues [11, 12], *polarity and charged value* of amino acids at position 2, 3, 5 and 6 [12], *molecular size* [13] and *entropy of peptides* [14]. In addition, two complex scores for *differential agretopicity index (DAI)* [15] and *amino acid pairwise contact potentials (AAPPs)* [16] were further considered. More detailed evidences and rationales for collected features are provided in Supplementary Data.

In addition to the 13 feature, we defined a new score, *a sequence similarity to known epitopes*, in light of a previous hypothesis between the similarity and immunogenicity [17, 18]. As the fundamental objective of the immune response is to distinguish non-self peptides from self, we assumed that these mutations could be prioritized by developing a proper measure. The 14 features are enlisted in Supplementary Table 1.

Construction of control positive and negative dataset

To construct the positive dataset (Supplementary Table 2), we initially collected 1,113 epitopes and their corresponding HLA alleles that were reported to exhibit positive T cell response in humans [10]. To find epitopes that can be generated by hypothetical somatic mutations in human genome, we compared the sequences of the 1,113 epitopes to those of the 20,198 reviewed Swiss-Prot human proteins [19] to only retain 311 epitopes whose sequences are differed from the best-match by up to two amino acids; the best-match protein was further used as a corresponding wild-type.

For negative dataset, we initially collected 22,245 variants from common (minor allele frequency [MAF] $\geq$0.05) non-synonymous single nucleotide polymorphisms (SNPs) from dbSNP v.141 with the assumption that widespread peptide variants would not lead to an immunogenic response. The HLA allele for negative dataset was randomly selected from HLA alleles of the positive set. To maintain the naturally occurring balance between positive and negative neopeptides (ratio, 1 to 48) [20], we randomly selected 14,633 out of the 22,245 mutant peptides to finalize the negative dataset.

Feature selection procedure

To achieve better classification accuracy and to reduce the risk of overfitting, we conducted feature selection from the 14 scores. Cleavage and TAP of the 14 scores were initially excluded due to the lack of consistency reported by a previous study [9]. For 12 remaining features, two major criteria were applied for selection: 1) informativeness of the feature in classification and 2) inter-dependency between features that causes redundancy.

To measure informativeness, three different analyses were used: correlation-based feature selection [21], information gain-based feature selection [22], and classification power achieved by a single feature. The single feature based classification power enables the prediction of the discriminative power of a feature in a trained machine learning classifier, which is represented by area under a curve (AUC) and area under a precision-recall curve (AUPRC). The final informativeness is measured by a merged score (Supplementary Figure S1A and Supplementary Table 3). Pearson and Spearman correlation were used to remove overlapping effects between inner individual features. If correlation between two features was higher than 0.8 in both methods, one was excluded. Finally, nine immunogenicity features: IC_{50}, rank, combined score, immunogenicity score, hydrophobicity, polarity&charged score, DAI, AAPPs and similarity were utilized to construct the machine-learning classifiers (see details in Supplementary Data and Supplementary Figure S2-6).

Machine learning-based classification for immunogenicity prediction

On the basis of the selected immunogenicity features, the machine learning-based classifiers were constructed for four learning models: Gaussian naïve Bayes (GNB), locally weighted naïve Bayes (LNB), random forest (RF), and support vector machine (SVM).

To evaluate classifiers, we used 500 iterations of 10-fold cross-validation on the constructed dataset and measured the performance. In the training step, calculated immunogenicity features of the dataset were fed into four classifiers. Then we validated the performance of four trained classifiers and conventional methods on the independent dataset.

RESULTS

Overall workflow of Neopepsee

The overall workflow is shown in Figure 1B. RNA-seq data and a list of somatic mutations are required for analysis. The HLA allele can be supplied as an optional input; otherwise, it can be inferred computationally from the RNA-seq data. For each non-synonymous somatic mutation,

affected peptides are calculated and prepared for further analysis (see details in Supplementary Data). Neopepsee classifies the potential neoantigens into three categories (high, medium, and low) with respect to the predicted immunogenicity, and reports the results along with 87 immunogenicity-related values, including conventional predictions (Supplementary Table 4), expression levels of neopeptides and immune regulatory genes (e.g., PD1, PD-L1).

Evaluation of neoantigen prediction in Neopepsee

Two types of descriptive statistics have been used to analyze the prediction accuracy of machine-learning classifiers (Figure 2). First, the overall AUC of the ROC curve was improved in Neopepsee (GNB: 0.975; LNB: 0.976; RF: 0.976; SVM: 0.981) compared to conventional measures (IC_{50}: 0.96; percentile rank: 0.946) in Figure 2A. Second, AUPRC (Figure 2B) was improved approximately 2 to 3-fold (GNB: 0.41; LNB: 0.44; RF: 0.68; and SVM: 0.61) compared with the IC_{50} (0.24) and percentile rank (0.28). Overall, the results demonstrate that machine learning-based classifiers have higher classification power than conventional single-value based approaches.

The overall accuracy at the specific threshold was measured. Conventional thresholds for immunogenicity prediction used 500nM for IC_{50} and 2.49 for percentile rank, respectively [2, 18, 23]. We divided the candidate neoantigens into three classes regarding the output membership probability of the trained classifiers: high (the most precise), medium (the most sensitive) and low. The lowest membership probability, which qualifies sensitivity level of 0.95 to exclude outliers, is set as threshold for medium class. The threshold for high class is the highest membership probability at which specificity is above 0.95. All other peptides were classified as the low class. As expected, high class had greatly increased precision and specificity with a slight loss of sensitivity in the test step, whereas the medium class was optimized for increased sensitivity.

In terms of AUC and AUPRC, the RF and SVM classifiers showed the best performance. However, the low thresholds at the membership probability in the medium class implied the perceptual tendency to call a smaller number of answers to prioritize specificity in both models. The tendency led to a drastic drop of precision at obtaining higher recall (Figure 2B). Therefore, LNB was finally selected as a classification model based on performance robustness.

Tests on independent experimental data

Neopepsee was tested on independent data sets from recent studies that reported experimentally confirmed immunogenic and non-immunogenic peptides in melanoma [23] and chronic lymphocytic

leukemia [24] patients (Figure 3). Both studies validated the induced T-cell responses experimentally using a MHC dextramer assay to evaluate vaccine-induced T cell responses [23] or a IFN-γ ELISPOT assay to measure spontaneous T cell responses [24]. From both studies, 1,093 peptides were obtained, 65 of which were validated (12 immunogenic and 53 non-immunogenic). The number of total calls and true/false positives was assessed in the medium and high classes of Neopepsee and further compared with the conventional criteria (Figure 3A and Supplementary Table 5).

Regarding sensitivity, IC_{50} and the medium class called all 12 answers: note that the perfect sensitivity for IC_{50} is expected, because the peptides for validation were initially selected by IC_{50}. Classification using percentile rank and the high class missed one and two answers, respectively. However, the high class only misclassified 14 non-immunogenic peptides out of the 53, increasing in specificity to 0.74 (compared to 0.45 of IC_{50} and 0.42 of percentile rank). The balanced measure (f-score) confirmed the improved classification power (0.41-0.45 in conventional criteria *vs.* 0.48-0.56 in Neopepsee).

For more accurate comparison of discriminative power, the distributions of scores were plotted for immunogenic and non-immunogenic peptide groups (Figure 3B). The *P*-value of discriminative power was calculated by Wilcoxon ranksum test. The results showed a tighter clustering of immunogenic peptides, with a better separation from non-immunogenic peptides (*P*-value, 6.84e-05). While the majority of non-immunogenic peptides are assigned with low probabilistic scores (<0.5), separation of false negatives with very high scores (~1.0) would be the key to achieving better separation, which we expect with continued accumulation of validated data for training.

Application to The Cancer Genome Atlas Stomach Adenocarcinoma (TCGA-STAD) dataset

We applied Neopepsee to a large cancer genome cohort. A total of 224 samples were analyzed, and 3,760 putative neoantigens were identified. The median of somatic single-nucleotide variants (SNV) was 49 and the median of putative neoantigens was 7 (Figure 4A). The number of somatic SNVs largely differed according to microsatellite instability (MSI) status (median of 452 in MSI-high, 56 in MSI-low, and 40 in microsatellite stable [MSS] tumors; Figure 4B). The number of neoantigens in MSI-high tumors (median, 68) was higher than that of MSI-low (median, 10) or MSS tumors (median, 5). Interestingly, tumors with neoantigens exhibited better prognosis compared to tumors without neoantigens (29.1 versus 14.1 months without neoantigens; log-rank *P*=0.024; Figure 4C). However, MSI status was not significantly associated with overall survival (29.4 versus 26.7 months with MSS; log-rank *P*=0.616; Figure 4D). Recently, Rooney, et al. calculated immune cytolytic activity scores as indicators of CD8+ T cell activation and showed neoantigens to be likely to induce cytolytic activity

[25]. In the cox-regression analysis, the absence of neoantigens and advanced tumor stage (III and IV) were identified as independent prognostic factors for overall survival (Figure 4E). The positivity of neoantigen was associated with improved overall survival in both univariate (hazard ratio, 3.1; *P*=0.022) and multivariate analysis (hazard ratio, 2.2; *P*=0.040). Our data suggest that increased neoantigen loads by microsatellite instability, not MSI status itself, may be a favorable prognostic factor. Of 3,760 neoantigens, only 16 (0.42%) were found in more than one tumor sample (Supplementary Table 6). We compared identified neoantigens with known immune epitopes. In addition to known H. *pylori* epitopes (n=7, Supplementary Figure S7A), we identified a total of 1,867 known immune epitopes (Supplementary Table 7). Most immune epitopes are derived from *Mycobacterium tuberculosis* (24%), *Trypanosoma cruzi* (19%), Vaccinia virus (6%), Human herpes virus (4%), and, Hepatitis C virus (2%), many of these bacteria/viruses can induce chronic inflammation, one of critical mediators of tumor development including gastric cancer (Supplementary Figure S7B).

DISCUSSION

Due to the great diversity, multi-step biochemical processes, and the stochastic nature of T-cell immune response, accurate prediction of neoantigen has been one of the most challenging problems in the immunoinformatics field. As we assumed, a single value associated with a part of the whole process can hardly provide sufficient information to resolve the complexity. In this context, systematic integration of multiple features into a unified workflow is urgently needed to increase the accuracy and to provide a sustainable framework that exploits the growing information. Notably, a recent study to predict MHC-I-binding peptides based on mass spectrometry shed light on identifying binding motifs and antigen processing rules [26]. We expect that such advances will reinforce Neopepsee through a continuous re-training of the machine learning classifier with updated data sets and feature selection.

One of the ultimate goals of neoantigen prediction software is to classify patients who will benefit from immunotherapy, or to design a personalized cancer vaccine. Recent studies showed that higher mutational burden was correlated with better anti-tumor activity of CTLA4 or PD-1 blockade [3, 4, 18]. Although the number of neopeptides generated by somatic mutation seemed to be important for predicting anti-tumor activity of immunotherapy, the criteria to identify neopeptides and the correlation were inconsistent across studies [3, 18]. Future studies identifying optimized selection criteria for neopeptides and further correlative analysis are warranted. Since most neoantigenic peptides are not identical between tumors [4], cancer vaccines targeting neopeptides may not be a ‘universal’ solution that provides broad coverage to cancer patients. Nevertheless, Neopepsee will

enable the efficient analysis of a personal somatic mutation profile and identification of potential neopeptides for personalized vaccination.

In summary, Neopepsee can be applied not only to identify putative neoantigens, but also to compare neoantigens with known immune epitopes. The analysis results can be used for subsequent prognostic/predictive biomarker discovery or to design antigens for cancer vaccines.

AVAILABILITY

The program is available at http://sourceforge.net/projects/neopepsee/.

ACKNOWLEDGEMENT

The authors thank Dong-Su Jang (Medical Illustrator, Department of Research Affairs, Yonsei University College of Medicine, Seoul, South Korea) for his help in creating the medical illustrations.

FUNDING

This work was supported by the Basic Science Research Program through the National Research Foundation of Korea (NRF) funded by the Ministry of Science, ICT & Future Planning [2015R1C1A1A01053638, 2013R1A3A2042197]; and the Korea Health Technology R&D Projects through the Korea Health Industry Development Institute (KHIDI) funded by the Ministry of Health & Welfare [HI14C1324], Republic of Korea. Sangwoo Kim was additionally funded by a faculty research grant from the Yonsei University College of Medicine [6-2016-0081].

DISCLOSURE

The authors have declared no conflicts of interest.

REFERENCES

1. York IA, Rock KL. Antigen processing and presentation by the class I major histocompatibility complex. Annu Rev Immunol 1996; 14: 369-396.
2. Brown SD, Warren RL, Gibb EA et al. Neo-antigens predicted by tumor genome meta-analysis correlate with increased patient survival. Genome Res 2014; 24: 743-750.

3. Van Allen EM, Miao D, Schilling B et al. Genomic correlates of response to CTLA-4 blockade in metastatic melanoma. Science 2015; 350: 207-211.
4. Rizvi NA, Hellmann MD, Snyder A et al. Cancer immunology. Mutational landscape determines sensitivity to PD-1 blockade in non-small cell lung cancer. Science 2015; 348: 124-128.
5. Neefjes J, Jongsma MLM, Paul P, Bakke O. Towards a systems understanding of MHC class I and MHC class II antigen presentation. Nature Reviews Immunology 2011; 11: 823-836.
6. Vita R, Overton JA, Greenbaum JA et al. The immune epitope database (IEDB) 3.0. Nucleic Acids Res 2015; 43: D405-412.
7. Hoof I, Peters B, Sidney J et al. NetMHCpan, a method for MHC class I binding prediction beyond humans. Immunogenetics 2009; 61: 1-13.
8. Trost B, Bickis M, Kusalik A. Strength in numbers: achieving greater accuracy in MHC-I binding prediction by combining the results from multiple prediction tools. Immunome Res 2007; 3: 5.
9. Stranzl T, Larsen MV, Lundegaard C, Nielsen M. NetCTLpan: pan-specific MHC class I pathway epitope predictions. Immunogenetics 2010; 62: 357-368.
10. Calis JJ, Maybeno M, Greenbaum JA et al. Properties of MHC class I presented peptides that enhance immunogenicity. PLoS Comput Biol 2013; 9: e1003266.
11. Chowell D, Krishna S, Becker PD et al. TCR contact residue hydrophobicity is a hallmark of immunogenic CD8+ T cell epitopes. Proc Natl Acad Sci U S A 2015; 112: E1754-1762.
12. Patronov A, Doytchinova I. T-cell epitope vaccine design by immunoinformatics. Open Biol 2013; 3: 120139.
13. Dintzis HM, Dintzis RZ, Vogelstein B. Molecular determinants of immunogenicity: the immunon model of immune response. Proc Natl Acad Sci U S A 1976; 73: 3671-3675.
14. Liu MK, Hawkins N, Ritchie AJ et al. Vertical T cell immunodominance and epitope entropy determine HIV-1 escape. J Clin Invest 2013; 123: 380-393.
15. Duan F, Duitama J, Al Seesi S et al. Genomic and bioinformatic profiling of mutational neoepitopes reveals new rules to predict anticancer immunogenicity. J Exp Med 2014; 211: 2231-2248.
16. Saethang T, Hirose O, Kimkong I et al. PAAQD: Predicting immunogenicity of MHC class I binding peptides using amino acid pairwise contact potentials and quantum topological molecular similarity descriptors. J Immunol Methods 2013; 387: 293-302.
17. Hoof I, Perez CL, Buggert M et al. Interdisciplinary analysis of HIV-specific CD8+ T cell responses against variant epitopes reveals restricted TCR promiscuity. J Immunol 2010; 184: 5383-5391.
18. Snyder A, Makarov V, Merghoub T et al. Genetic basis for clinical response to CTLA-4 blockade in melanoma. N Engl J Med 2014; 371: 2189-2199.
19. Apweiler R, Bairoch A, Wu CH et al. UniProt: the Universal Protein knowledgebase. Nucleic Acids Res 2004; 32: D115-119.
20. Schumacher TN, Schreiber RD. Neoantigens in cancer immunotherapy. Science 2015; 348: 69-74.
21. Hall MA. Correlation-based feature selection of discrete and numeric class machine learning. 2000.
22. Azhagusundari B, Thanamani AS. Feature selection based on information gain. International Journal of Innovative Technology and Exploring Engineering (IJITEE) 2013; 2: 18-21.
23. Carreno BM, Magrini V, Becker-Hapak M et al. Cancer immunotherapy. A dendritic cell vaccine increases the breadth and diversity of melanoma neoantigen-specific T cells. Science 2015; 348: 803-808.
24. Rajasagi M, Shukla SA, Fritsch EF et al. Systematic identification of personal tumor-specific neoantigens in chronic lymphocytic leukemia. Blood 2014; 124: 453-462.
25. Rooney MS, Shukla SA, Wu CJ et al. Molecular and genetic properties of tumors associated with local immune cytolytic activity. Cell 2015; 160: 48-61.
26. Abelin JG, Keskin DB, Sarkizova S et al. Mass Spectrometry Profiling of HLA-Associated Peptidomes in Mono-allelic Cells Enables More Accurate Epitope Prediction. Immunity 2017; 46: 315-326.

FIGURES LEGENDS

Figure 1. MHC-I antigen presentation pathway and corresponding Neopepsee procedure.

(A) The mutant peptide (mutation sequence represented in red) from a tumor-specific antigen can be present in the plasma membrane of the major histocompatibility complex (MHC)-I molecule as the result of a series of reactions. First, tumor-specific antigens are degraded by the proteasome (Process 1). Then, the resulting peptides are transported via transporters associated with antigen presentation (TAP) into the endoplasmic reticulum (ER) lumen. The neopeptide binds to the binding-groove of MHC-I molecules (Process 2). Peptide-MHC class I complexes (pMHC-I) are then transported via the endoplasmic reticulum (ER)-Golgi pathway to the plasma membrane for antigen presentation to activate CD8+ T cells. MHC-I, major histocompatibility complex I; β2m, β2-microglobulin; TCR, T cell receptor. (B) Overall Neopepsee workflow. Somatic mutations and gene expressions of a given tumor tissue are assessed for neoantigen prediction. In total, 10 immunogenicity features are calculated for each mutant neopeptide and fed into a classifier. Yellow boxes denote unique modules in Neopepsee.

Figure 2. Performance evaluation for Neopepsee.

(A) ROC curves of four predictive models (Gaussian naïve Bayes, locally weighted naïve Bayes, random forest, and support vector machine,) and two conventional methods (IC50 and percentile rank). All four predictive models outperformed the conventional methods. (B) pROC curves of the same six models. All four predictive models show better performance than the conventional methods. AUPRC is maximized in the RF model, however, an acute drop in the high recall area is observed; LNB shows the best performance when the recall was 1. GNB=Gaussian naïve Bayes, LNB=locally weighted naïve Bayes, RF=random forest, SVM=support vector machine, RANK=percentile rank, High/Medium=classified with high/medium probability for immunogenicity. MCC=Matthews correlation coefficient.

Figure 3. Performance of Neopepsee in independent validation data sets.

(A) Comparison of performances between each method. # of calls, the total neoantigen candidates from the each method; # of hits, the number of true positives; # of FPs, the number of false positives. (B) Comparison of discriminative power for three methods. Only Neopepsee shows significance between immunogenic and non-immunogenic scores. The y-axis of Neopepsee was vertically inverted for convenient comparison.

Figure 4. Application of Neopepsee to stomach adenocarcinoma (TCGA-STAD) dataset.

(A) The number of putative neoantigens and somatic point mutations in TCGA-STAD tumors (N = 224). (B) The number of somatic point mutations according to microsatellite instability (MSI) status in TCGA-STAD tumors (N = 224). (C) Kaplan-Meier estimates of overall survival according to the positivity of neoantigens. (D) Kaplan-Meier estimates of overall survival according to the MSI status. (E) Univariate and multivariate Cox regression survival analyses.

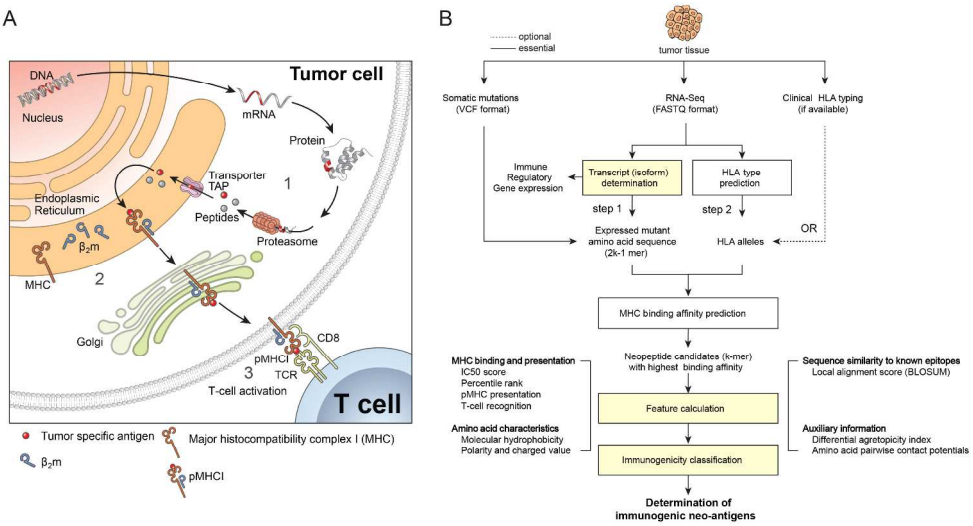

Figure 1. MHC-I antigen presentation pathway and corresponding Neopepsee procedure. (A) The mutant peptide (mutation sequence represented in red) from a tumor-specific antigen can be present in the plasma membrane of the major histocompatibility complex (MHC)-I molecule as the result of a series of reactions. First, tumor-specific antigens are degraded by the proteasome (Process 1). Then, the resulting peptides are transported via transporters associated with antigen presentation (TAP) into the endoplasmic reticulum (ER) lumen. The neopeptide binds to the binding-groove of MHC-I molecules (Process 2). Peptide-MHC class I complexes (pMHC-I) are then transported via the endoplasmic reticulum (ER)-Golgi pathway to the plasma membrane for antigen presentation to activate CD8+ T cells. MHC-I, major histocompatibility complex I; β2m, β2-microglobulin; TCR, T cell receptor. (B) Overall Neopepsee workflow. Somatic mutations and gene expressions of a given tumor tissue are assessed for neoantigen prediction. In total, 10 immunogenicity features are calculated for each mutant neopeptide and fed into a classifier. Yellow boxes denote unique modules in Neopepsee.

289x157mm (300 x 300 DPI)

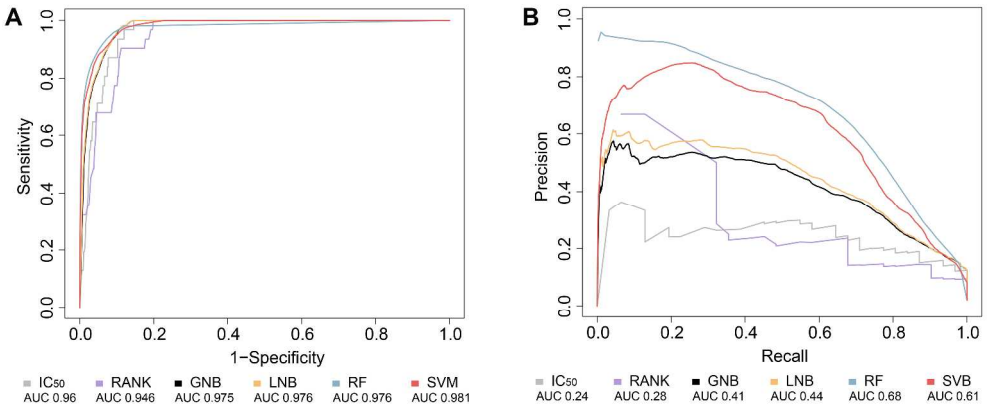

Figure 2. Performance evaluation for Neopepsee.
(A) ROC curves of four predictive models (Gaussian naïve Bayes, locally weighted naïve Bayes, random forest, and support vector machine,) and two conventional methods (IC50 and percentile rank). All four predictive models outperformed the conventional methods. (B) pROC curves of the same six models. All four predictive models show better performance than the conventional methods. AUPRC is maximized in the RF model, however, an acute drop in the high recall area is observed; LNB shows the best performance when the recall was 1. GNB=Gaussian naïve Bayes, LNB=locally weighted naïve Bayes, RF=random forest, SVM=support vector machine, RANK=percentile rank, High/Medium=classified with high/medium probability for immunogenicity. MCC=Matthews correlation coefficient.

439x184mm (300 x 300 DPI)

A

	IC50	RANK	Neopepsee	
	≤500nM	≤2.49	medium	high
# of calls	283	184	259	197
# of hits	12	11	12	10
# of FPs	29	31	26	14
Sensitivity	1.00	0.92	1.00	0.83
Specificitiy	0.45	0.42	0.51	0.74
F-score	0.45	0.41	0.48	0.56

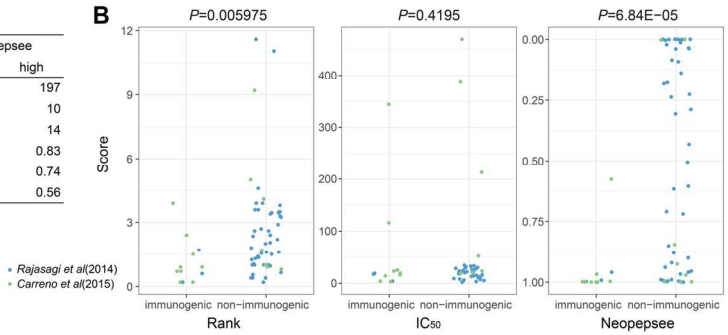

Figure 3. Performance of Neopepsee in independent validation data sets.
(A) Comparison of performances between each method. # of calls, the total neoantigen candidates from the each method; # of hits, the number of true positives; # of FPs, the number of false positives. (B) Comparison of discriminative power for three methods. Only Neopepsee shows significance between immunogenic and non-immunogenic scores. The y-axis of Neopepsee was vertically inverted for convenient comparison.

152x52mm (300 x 300 DPI)

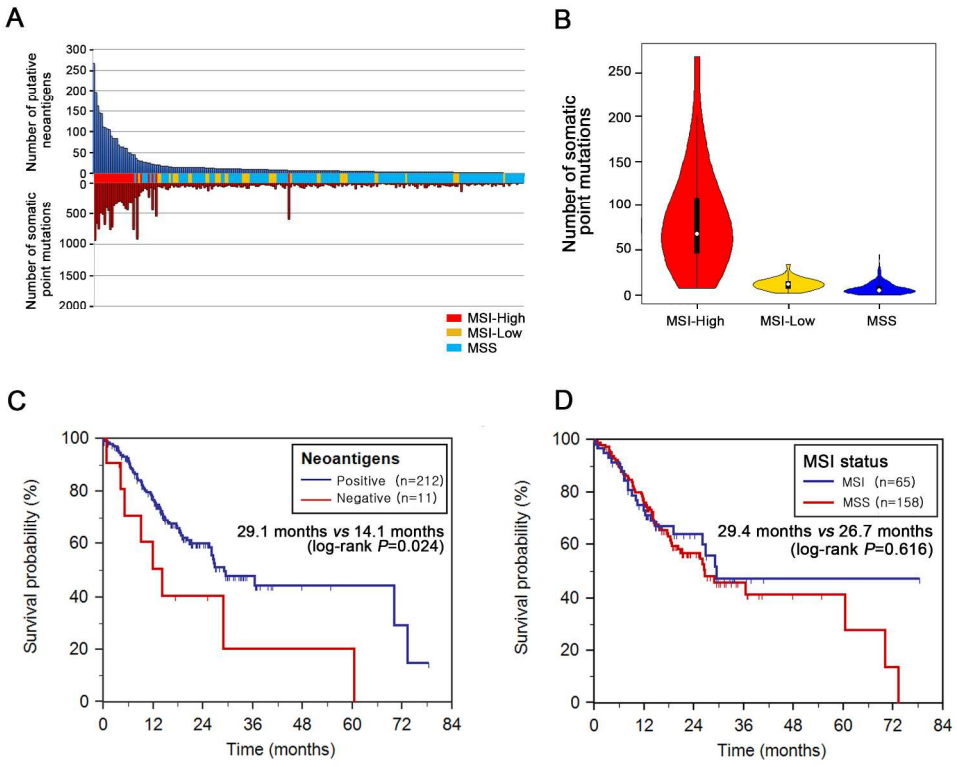

E

Variable	Category	Univariate analysis			Multivariate analysis		
		HR	95% CI	*P*	HR	95% CI	*P*
Neoantigens	negative *v* positive (ref)	3.1	1.18 to 8.47	0.022*	2.2	1.04 to 4.82	0.040*
Stage	III, IV *v* I, II (ref)	2.4	1.14 to 5.08	0.021*	2.0	1.25 to 3.16	0.004*
Sex	female *v* male (ref)	0.9	0.44 to 2.10	0.923	1.1	0.72 to 1.86	0.545
Age	≥65 *v* <65 (ref)	1.1	0.73 to 1.76	0.571	1.0	0.66 to 1.63	0.878
Cytolytic activity (Rooney, et al)	high *v* low (ref)	0.8	0.52 to 1.30	0.398	0.8	0.49 to 1.25	0.306
Microsatellite instability (MSI)	MSI *v* MSS (ref)	0.9	0.54 to 1.43	0.617	1.0	0.61 to 1.65	0.989

*P-values <0.05; HR, hazard ratio; CI, confidence interval; MSS, microsatellite stable

Figure 4. Application of Neopepsee to stomach adenocarcinoma (TCGA-STAD) dataset.
(A) The number of putative neoantigens and somatic point mutations in TCGA-STAD tumors (N = 224). (B) The number of somatic point mutations according to microsatellite instability (MSI) status in TCGA-STAD tumors (N = 224). (C) Kaplan-Meier estimates of overall survival according to the positivity of neoantigens. (D) Kaplan-Meier estimates of overall survival according to the MSI status. (E) Univariate and multivariate Cox regression survival analyses.

239x279mm (300 x 300 DPI)